Desalination and Water Treatment
www.deswater.com

doi:10.5004/dwt.2019.23092

139 (2019) 123–132
January

Using a multi-objective optimal design of GMDH type neural networks to evaluate the quality of treated water in a water treatment plant

Fereshteh Alitaleshi, Allahyar Daghbandan*

Department of Chemical Engineering, Faculty of Engineering, University of Guilan, Guilan, Iran, Tel. +989112937219, email: taleshi.fereshteh@gmail.com (F. Alitaleshi), Tel. +989111318785, email: daghbandan@guilan.ac.ir (A. Daghbandan)

Received 22 February 2018; Accepted 8 September 2018

ABSTRACT

In this research, a model based on the multi-objective optimal design of GMDH[1]-type neural network is proposed for evaluating the quality of treated water. To validate the proposed model, a case study was carried out based on the data sets obtained from Rasht Water Treatment Plant (WTP), Guilan, Iran. For modeling, the experimental data obtained from the laboratory and operation unit were divided into training and testing groups (70% for training and 30% for testing). After modeling, the predicted values were compared with the ones obtained from the experimental values. The determination coefficient of the predicted values for the two data sets of GMDH model (laboratory and operation unit) were 0.9905 and 0.9714 respectively. Comparison between experimental and mathematical results from GMDH-type neural networks showed the success of this method.

Keywords: Drinking water treatment; Water quality; Residual turbidity; Modelling; Optimization; GMDH- type NN

1. Introduction

Safe water with proper quality is necessary for life. The quality of drinking water is very important, because water with low quality may cause health-related and economic problems which have a major impact on people's daily lives. The drinking water should be properly treated and disinfected before drinking; thus it should be totally clean, pure and free of any disease-causing microbes [1].

There are many parameters to measure the quality of water including turbidity. Turbidity is commonly used as an index of the general condition of drinking water and an index of the efficiency of coagulation, disinfection and filtration processes in drinking water treatment; therefore it is an important operational parameter and should be minimized. Also, many variables influence it [2,3].

Turbidity is a main physical characteristic of water which is caused by suspended particles or colloidal matter [4]. It is measured using nephelometric turbidity units (NTU). However, turbidity should not be more than 1 NTU and ideally much lower to 0.5 NTU, before disinfection and at all times. Also, Turbidity of water after jar test should be less than 5 NTU [2,4,5].

The removal of turbidity is a very important part of water treatment. Turbidity can be affected by the physical, microbiological, chemical and radiological characteristics of raw water [6]. Electrolytic conductivity is a useful test in raw water for determination of minerals. Other important parameters that have a remarkable influence on the removal of water turbidity are chemical material dosages such as coagulants and disinfectants. Temperature [7–10], pH [8–11], alkalinity [7,11], color and suspended solids [12]of the raw water can have a considerable effect on coagulation and flocculation [7,11]. Coagulants or polyelectrolytes do not fully inactivate viruses. Therefore, for a safe drinking water, disinfection of water is required [13].

In WTP, coagulation and flocculation are essential components of treatment processes for removal of turbidity

*Corresponding author.

[1]Group Method of Data Handling

from drinking water [5]. Unusual condition, such as heavy rains, the storm water, seasonal variations cause raw water turbidity variations.

Determination of treated water turbidity which is calculated experimentally or operators' own experience by using trial and error in material injection is performed, so that the water quality is not uniform due to human mistake and the inaccuracy of the amount of injected material. Hence, determining the optimal dosage of material is necessary and it is vital to maintain economic plant operation such as reducing man power and expensive chemical costs. Traditionally, jar tests in laboratory and operators' own experience in operation unit are used to determine the optimum material dosage. Also, jar test simulates the coagulation and flocculation processes in WTPs [13–15]. This makes the water treatment more effective, easy, and economical. However, jar tests are time-consuming, relatively expensive [16–21] and cannot be used to respond to rapid changes in raw water quality [22–25] and thus are not suitable for real-time control [20]. As a result, jar tests are generally carried out periodically [19,20].

Monitoring and controlling water treatment processes are challenging task because of their complexity, nonlinearity, and numerous contributory variables. Therefore modeling water quality has become more important in recent years [1].

Nowadays, many studies are being performed on water treatment process. Neural networks as an artificial intelligence are considered as suitable tools for prediction of properties compared to usual correlations. Since they are non-parametric statistical modeling tools, they do not require pre-assumption of the input-output relationship and are able to correlate parameters with any possible complexity [26].

In some previous studies, ANN[2]s were used to determine the optimal dosage of alum by the applied number of raw water quality parameters as model inputs for WTP [14,22,25,27,28]. Also,Baxter et al. [19] developed a similar model for the removal of natural organic matter (NOM) by enhanced coagulation at the Rossdale WTP in Canada.

Nowadays, many studies are being performed on evaluating the water quality. For example, Reckhow [29] presented the Bayesian probability networks for surface water quality assessment and prediction in the Neuse River estuary in North Carolina. Baxter et al. [30] developed the ANN models for modeling and control water quality in drinking WTP in Edmonton, Alberta. Also, Pike [31] used a probabilistic Bayesian network to model compliance violations in drinking water treatment by environmental and system characteristics in Pennsylvania. The model indicated that the operator decisions such as coagulant dosage and filter back wash frequency play the greatest role in determining the violation likelihood on drinking water quality. Juntunen et al. [1] used the linear (MLR[3]) and nonlinear (MLP[4]) modeling methods to both residual turbidity and alum modeling in a water treatment process. The results showed the goodness of the MLP model was slightly better than that of the MLR in both cases.

In all of the above studies, the presented models showed a good agreement with the experimental results, but the disadvantage of most of them was the inability to respond to changes in the desired levels of the raw water parameters. Here the researchers tried to present a model that can overcome this deficiency. For example, Adaptive Neuro-Fuzzy Inference System (ANFIS) method [27] and Neuro-Fuzzy GMDH model has been reported in [32–36] also, The GMDH network with Back Propagation algorithm has been presented in [37–40]; According to the comparisons, the ANFIS technique could be employed successfully in modeling coagulant dosage from the available raw water data. Recently, Daghbandan et al. [41] developed the GMDH-Type NN and MOGA[5] for modeling and optimization of poly electrolyte dosage at Guilan WTP in Iran. To the comparison between the results of modeling and the experimental data showed that the use of GMDH-type NN networks is a very suitable replacement for jar test.

The method suggested here for modeling and predicting the residual turbidity in treated water using both operating and laboratory data sets in order to evaluate the quality of drinking water in WTP, is the multi-objective optimal design of GMDH-type NN [42,43]. The residual turbidity in water depends on raw water parameters such as temperature, pH, turbidity, suspended solids, electrolytic conductivity and chemicals dosages such as coagulants and disinfectants. During this study, aluminum sulfate and poly electrolyte were used as the coagulant and coagulant aid, respectively.

Ultimately, the genetic algorithms (GA) are used for optimization of influence parameters on the removal of turbidity in water treatment process.

2. Methodology

2.1. Case study

This study was performed in both laboratory – using jar test apparatus (AL50, AQUALYTIC, Germany) – and operation units in WTP. The Great WTP has located approximately at 20 km from Rasht city in Guilan Province, Iran, which supplies potable water to Rasht neighborhood areas with the capacity of 6,000 L/s and its raw water was obtained from Shahrebijar and Sefidrood rivers the water quality of which is subject to seasonal changes. The treatment essentially consists of preliminary disinfection, primary sedimentation, coagulation, flocculation, secondary sedimentation, filtration and final disinfection. Then, the water is stored and ready for distribution.

2.2. Data collection

In order to obtain the input/output data required to develop and validate the GMDH models, the experimental data were obtained from the jar test in laboratory unit over a period of 10 months (from August 2015 to June2016). The inputs of the model were measured by different apparatus, including temperature (340i, WTW, Germany), pH (340i, WTW, Germany), turbidity (2100N, HACH, USA) and electrolytic conductivity (330i, WTW, Germany) of the raw

[2]Artificial Neural Network
[3]Multiple Linear Regression
[4]Multi-Layer Perceptron
[5]Multi-Objective Genetic Algorithms

water, chemicals dosage including aluminum sulfate and polyelectrolyte dosage and the output of model was residual turbidity after jar test for each test. A total of 150 data sets were collected.

In addition, for operation unit modeling, the operating data were selected from the Guilan WTP data bank during a period of about 18 months (from March 2014 to September 2015) randomly. The inputs of the model were including temperature, pH, suspended solids of the raw water and chemicals dosage including aluminum sulfate and poly electrolyte dosage as coagulants and disinfectant dosage in primary (pre-chlorination) and secondary (pass-chlorination) disinfection and the output of model was residual turbidity of the treated water. A total of 721 data sets were collected. The data range for laboratory and operating variables are shown in Table 1.

2.2.1. Jar test

In this study, the jars were filled with raw water sample (1000 mL) for the jar test and then different dosages of the aluminum sulfate (as coagulant) were added to each jar. The samples were mixed under rapid mixing condition (169–170 rpm) for 1 min and 18 s. The rapid mix helps to disperse the coagulant throughout each container. Then the apparatus was set to slow mixing (109–111 rpm) for 6 min. This slower mixing speed helps promote floc formation by enhancing particle collisions, which leads to the formation of larger flocs. Then different dosages of the coagulant aid (polyelectrolyte) were added to each jar and mixing was continued for 2 min with the same speed. After mixing the samples left for 30 min in order to settle the sediments,the samples were collected from about 3 cm below the surface in each jar and residual turbidity was measured by a turbidimeter. And finally, the coagulant dosages with the lowest residual turbidity were determined as the optimum coagulant dosages.

2.3.Division of data

The raw water database including six input variables (temperature, pH, turbidity, electrolytic conductivity, aluminum sulfate and polyelectrolyte dosage) for laboratory data set and seven input variables (temperature, pH, suspended solids, aluminum sulfate and polyelectrolyte dosage, primary and secondary chlorination dosage) for operating data set (see Table 1) were used to model residual turbidity in treated water.

Before modeling, the outliers in the data were filtered out manually. For modeling, the data sets were divided into two subsets: 70% of the total number of samples was used for training the model, and validation data sets consisting of the remaining 30% of the samples were applied for testing to show the prediction ability of such a developed GMDH model during the training process.

2.4. GMDH Type - Neural network

Using the GMDH algorithm, a model can be represented as a set of neurons in which different pairs of them in each layer are connected through a quadratic polynomial and, therefore, produce new neurons in the next layer. Such representation can be used in modeling to map inputs to outputs. The formal definition of the identification problem is to find a function, that can be approximately used instead of the actual one, *f*, In order to predict output for a given input vector $X = (x_1, x_2, x_3,\ldots, x_n)$ as close as possible to its actual output y. Therefore, given a number of observations (M) of multi-input, single output data pairs so that:

$$y_i = f\left(x_{i1}, x_{i2}, x_{i3},\ldots, x_{in}\right)\left(i = 1,2,..,M\right) \tag{1}$$

It is now possible to train a GMDH-type-NN to predict the output values for any given input vector = $(x_{i1}, x_{i2}, x_{i3},\ldots, x_{in})$, that is,

$$\hat{y}_i = \hat{f}\left(x_{i1}, x_{i2}, x_{i3},\ldots, x_{in}\right)\left(i = 1,2,3,\ldots,M\right) \tag{2}$$

In order to determine a GMDH type-NN, the square of the differences between the actual output and the predicted one is minimized, that is

$$\sum_{i=1}^{M}\left[\hat{f}\left(x_{i1}, x_{i2},\ldots, x_{in}\right) - y_i\right]^2 \to \min \tag{3}$$

Table 1
The data range of laboratory and operating variables for GMDH modeling

Model	Variables [unit]	Laboratory data			Operating data		
		Min	Max	Average	Min	Max	Average
Inputs	Temperature [°C]	3.9	25.4	16.35	3.9	28.8	17.11
	pH	7.88	8.45	8.22	7.5	8.5	8.02
	Suspended solids [mg/l]	–	–	–	4	680	77.57
	Electrical conductivity [µs/cm]	148	1737	78	–	–	–
	Turbidity [NTU]	4.7	990	56.88	–	–	–
	Primary chlorination [ppm]	–	–	–	2.216	5.727	3.698
	Aluminum sulfate [ppm]	7	48	10.6	3.989	27.128	12.134
	Polyelectrolyte [ppm]	0.11	0.3	0.145	0.072	0.263	0.163
	Secondary chlorination [ppm]	–	–	–	0.22	2.99	1.293
Output	Residual turbidity [NTU]	1.12	3.95	1.98	0.4	1.6	0.67

The general connection between the inputs and the output variables can be expressed by a complicated discrete form of the Volterra functional series [42] in the form of:

$$y = a_0 + \sum_{i=1}^{n} a_i x_i + \sum_{i=1}^{n}\sum_{j=1}^{n} a_{ij} x_i x_j + \sum_{i=1}^{n}\sum_{j=1}^{n}\sum_{k=1}^{n} a_{ijk} x_i x_j x_k + \ldots, \quad (4)$$

Where is known as the Kolmogorov-Gabor polynomial [44]. The general form of mathematical description can be represented by a system of partial quadratic polynomials consisting of only two variables (neurons) in the form of:

$$\hat{y} = G\left(x_i, x_j\right) = a_0 + a_1 x_i + a_2 x_j + a_3 x_i^2 + a_4 x_j^2 + a_5 x_i x_j \quad (5)$$

In this way, such partial quadratic description is recursively used in a network of connected neurons to build the general mathematical relation of the inputs and output variables given in Eq. (4). Then, coefficients a_i in Eq. (5) are calculated using regression techniques. It can be seen that a tree of polynomials is constructed using the quadratic form given in Eq. (5). in this way, the coefficients of each quadratic function G_i are obtained to fit optimally the output in the whole set of input-output data pairs, that is,

$$E = \frac{\sum_{i=1}^{M} (y_i - G_i())^2}{M} \rightarrow \min \quad (6)$$

In the basic form of the GMDH algorithm, all the possibilities of two independent variables out of the total n input variables are taken in order to construct the regression polynomial in the form of Eq. (5) that best fits the dependent observations (y_i, $i = 1,2,3,\ldots,M$) in a least squares sense [45].

Using the quadratic sub-expression in the form of Eq. (5) for each row of M data triples, the following matrix equation can be readily obtained as:

$$Aa = Y \quad (7)$$

Where a is the vector of unknown coefficients of the quadratic polynomial in Eq. (5),

$$a = \left\{a_0, a_1, a_2, a_3, a_4, a_5\right\} \quad (8)$$

$$Y = \left\{y_1, y_2, y_3, \ldots, y_M\right\}^T \quad (9)$$

Here Y is the vector of the output's value from observation. It can be readily seen that:

$$A = \begin{bmatrix} 1 & x_{1p} & x_{1q} & x_{1p}^2 & x_{1q}^2 & x_{1p}x_{1q} \\ 1 & x_{2p} & x_{2q} & x_{2p}^2 & x_{2q}^2 & x_{2p}x_{2q} \\ \vdots & \vdots & \vdots & \vdots & \vdots & \vdots \\ 1 & x_{Mp} & x_{Mq} & x_{Mp}^2 & x_{Mq}^2 & x_{Mp}x_{Mq} \end{bmatrix} \quad (10)$$

The least squares technique from multiple regression analysis leads to the solution of the normal equations in the form of:

$$a = \left(A^T A\right)^{-1} A^T Y \quad (11)$$

which determines the vector of the best coefficients of the quadratic Eq. (5) for the whole set of M data triples.

3. Results and discussion

3.1. Multi-objective optimal design of GMDH-Type neural networks

In this research, group method of data handling (GMDH) type neural network has been used for prediction of residual turbidity in treated water – in both laboratory and operation unit - in Guilan WTP. A multi-objective uniform diversity genetic algorithm (MUGA) has been presented in [46–48] which will also be used in this study to design the parameters of GMDH model optimally. Structural parameters of the Pareto genetic design of GMDH-type NN are presented in Table 2.

Attempts have been made in the literature to use SNE[6] as a linear optimization technique (Eq. (11)) to recognize the parameters of the Volterra functional series (Eq. (5)). Y_i is optimally selected by GA, which is a number of the neuron.

Therefore, there is no single optimal solution as the best with relation to all the objective functions. Instead, there is a set of optimal solutions, known as Pareto optimal solutions or Pareto front for multi-objective optimization problems.

In this way, training and testing errors are chosen for the bi-objective Pareto optimization approach of GMDH models [Eq. (12)] using the methodology explained in detail in [47,49]. Consequently, in this paper, a hybridization of genetic algorithms and SNE are applied for the optimal design of GMDH model. The method suggested by some author in [47,49] is adopted here for optimal design of GMDH network for modeling of residual turbidity in treated water in WTP.

3.2. GMDH modeling and optimization of the experimental data

The Residual turbidity in treated water was used as desired outputs of the GMDH network. The feed-forward GMDH-type NN was devised for the residual turbidity that was constructed using experimental and operating data sets. The results obtained with the GMDH-type NN are presented in Tables and figures.

Fig. 1 and Fig. 2 depict the Pareto optimal solutions of both training and testing (or prediction) errors of GMDH model for the deterministic input-output data table. Points A and B stand for GMDH model with the least prediction and training errors respectively. Design point M, however, depict the trade off between such models which can be reasonably chosen as an optimal model compromisingly.

The GMDH values of training and prediction errors of deterministic optimal design point A, B, and M, are given in Table 3. The optimal structures of the proposed neural network with 4-hidden layers for both models are shown in Figs. 3 and 4. For example,"13152235154416352656353633363435" are corresponding chromosomes representations for the prediction of residual turbidity in laboratory unit (Table 4). In which, 1, 2, 3, 4, 5, and 6 stands for effective parameters on residual turbidity includes T, pH, Tu, EC, Alum and Poly electrolyte dosage in laboratory unit. The Pareto genetic design of GMDH-type NN provides an automated selection of essential input variables and builds polynomial equa-

[6]Solve Normal Equation

Table 2
Structural parameters of Pareto genetic design of GMDH-Type NN

Population size	400	Probability of crossover	0.97
Number of iteration	1200	Number of objective functions	2
Probability of mutation	0.09	Number of hidden layers	4

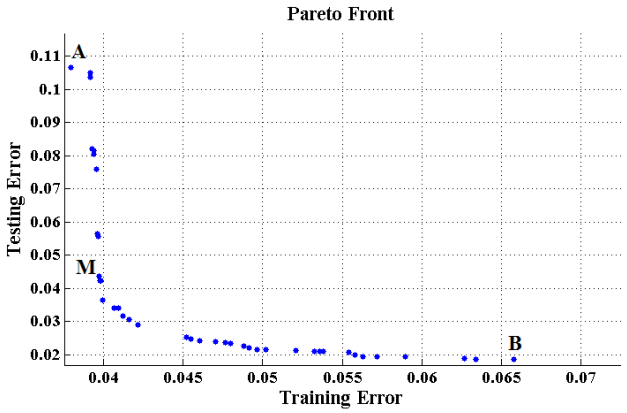

Fig. 1. Pareto optimal solutions of GMDH-type NN model in jar test data set for modeling of residual turbidity in treated water.

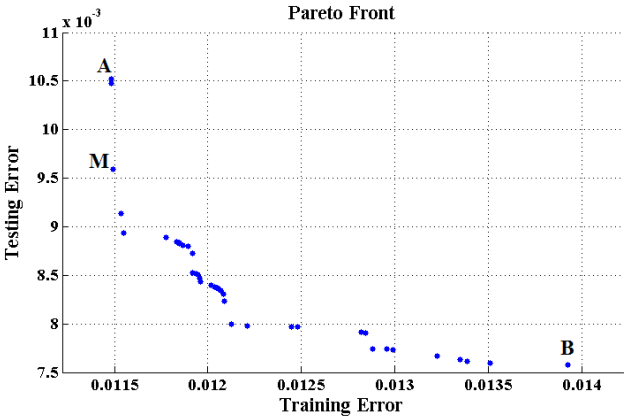

Fig. 2. Pareto optimal solutions of GMDH-type NN model in operation unit data set for modeling of residual turbidity in treated water.

Table 3
Training and prediction error of design point in deterministic approaches

Design point	Laboratory unit model		Operation unit model	
	TE	PE	TE	PE
A	0.03793	0.106436	0.013484	0.014941
B	0.065795	0.018469	0.015492	0.010708
M	0.039795	0.042199	0.013557	0.01376

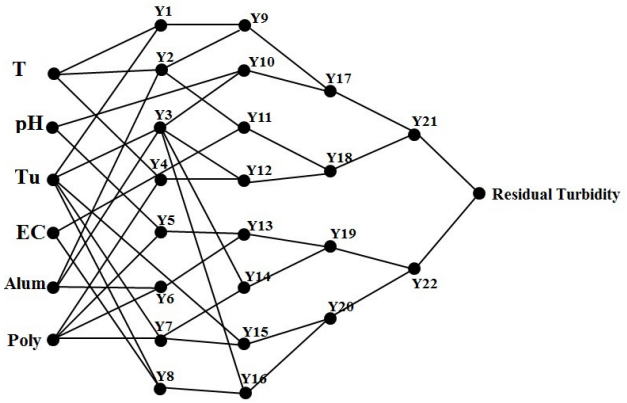

Fig. 3. Proposed structure of GMDH-type NN model for prediction of residual turbidity in laboratory unit (jar tests).

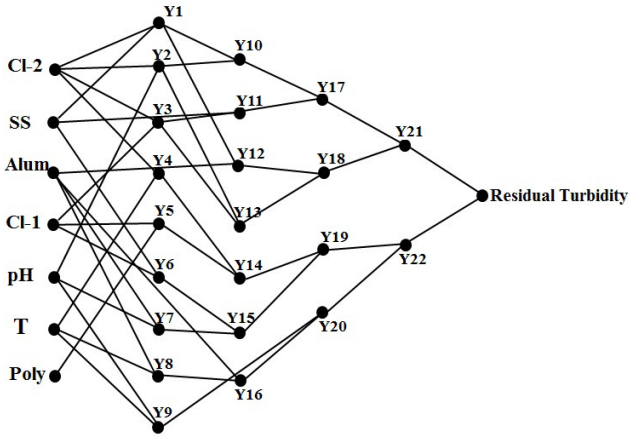

Fig. 4. Proposed structure of GMDH-type NN model for prediction of residual turbidity in operation unit.

Table 4
Optimal chromosomes for prediction of residual turbidity in treated water

Unit	Optimal chromosomes
Laboratory	131522351544163526563533633363435
Operation	12151422123314151647243533365656

tions for the residual turbidity modeling. These polynomial equations show the quantitative relationship between input and output variables. Y is an index of neurons.

To measure the model performance, a comparison is made between the experimental and the predicted values is shown in Figs. 5 and 6. In order to, the results of the developed models show a close agreement between experimental and predicted values of the models. In order to estimate the residual turbidity, parameters values were obtained by MUGA and SNE method (Tables 5 and 6).

In order to determine the accuracy of the model, the statistical measures are given in Table 7. These statistical

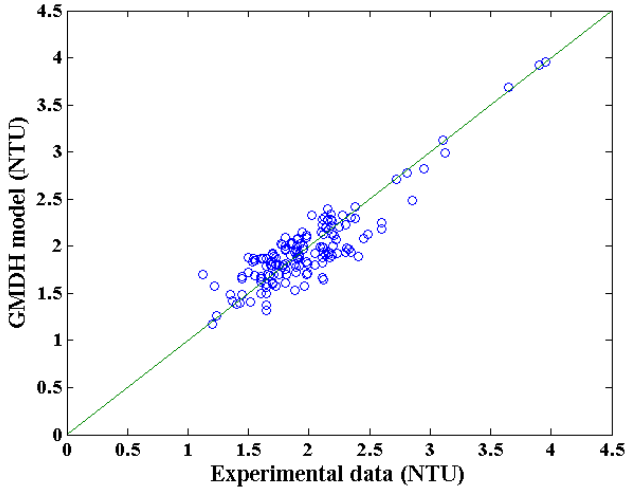

Fig. 5. Comparison between predictions of the model and actual data for residual turbidity in laboratory unit.

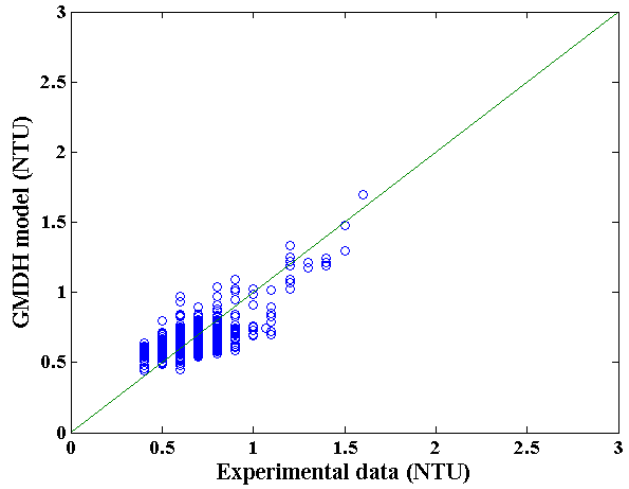

Fig. 6. Comparison between predictions of the model and actual data for residual turbidity in operation unit.

parameters including mean square error (MSE), normalized root-mean square error (NRMSE), average absolute deviation percent (AADP%), scatter index (SI) [50], BIAS and coefficient of determination (R^2) are used. The equations to compute the above parameters are as follows:

$$MSE = \frac{1}{n}\sum_{i=1}^{n}\left(Y_{(i,\exp)} - Y_{(i,\mathrm{mod}\,el)}\right)^2 \quad (12)$$

$$NRMSE = \left[\frac{1}{n}\left(\sum_{i=1}^{n}\left(Y_{(i,\exp)} - Y_{(i,\mathrm{mod}\,el)}\right)^2\right)\right]^{0.5} / \left(Y_{(\exp,\max)} - Y_{(\exp,\min)}\right) \quad (13)$$

$$AADP(\%) = \frac{100}{n}\sum_{i=1}^{n}\left|\left(\frac{Y_{(i,\mathrm{mod}\,el)}}{Y_{(i,\exp)}}\right)_i - 1\right| \quad (14)$$

$$SI = \sqrt{\frac{1}{n}\left(\sum_{i=1}^{n}\left(\left(Y_{(i,\mathrm{mod}\,el)} - \bar{Y}_{\mathrm{mod}\,el}\right) - \left(Y_{(i,\exp)} - \bar{Y}_{\exp}\right)\right)^2\right)} / \left(\frac{1}{n}\sum_{i=1}^{n}Y_{(i,\exp)}\right) \quad (15)$$

$$BIAS = \frac{1}{n}\sum_{i=1}^{n}\left(Y_{(i,\mathrm{mod}\,el)} - Y_{(i,\exp)}\right) \quad (16)$$

$$R^2 = 1 - \left[\sum_{i=1}^{n}\left(Y_{(i,\exp)} - Y_{(\mathrm{i,model})}\right)^2 / \sum_{i=1}^{n}\left(Y_{(\mathrm{i,exp})}\right)^2\right] \quad (17)$$

where $Y_{i,model}$ is the residual turbidity computed by the GMDH model, $Y_{i,exp}$ is the residual turbidity obtained by the experimental data, $\bar{Y}_{\mathrm{model}}$, $\bar{Y}_{\exp}$ refer to average of model and experimental data and $Y_{exp,max}$, $Y_{exp,min}$ and n refer to the maximum and minimum of experimental data and number of data set, respectively.

Finally, genetic algorithms are used to optimize the influence parameters for the removal of turbidity in drinking water treatment. Optimize parameters values that influence the removal of turbidity at laboratory and operation units are presented in Table 8. The effect of coagulants dosage on the removal of turbidity in optimum condition has been shown in Figs. 7 and 8. In these figures, the values of the other parameters are its optimum (Table 8).

Figs. 7 and 8 indicate that with increasing coagulants dosage includes i.e. aluminium sulfate and poly electrolyte, residual turbidity is decreased. Also, in optimum conditions, the amount of aluminium sulfate injection is more effective in turbidity removal than polyelectrolyte dosage. Also, excessive consumption of coagulants can increase the turbidity in water which is clear in both figures.

4. Conclusions

According to this research, the following conclusions are obtained:

In the present study, the Multi-objective optimal design of GMDH-Type NN was used for modeling and predicting the residual turbidity in treated water in both laboratory and operation units of WTP of Guilan, Iran.

The total numbers of experimental data of laboratory and operation units were 150 and 721 samples, respectively;including six and seven input variables, respectively, and both outputs represented the residual turbidity in treated water. The raw water datasets were divided into training and testing data sets.

GMDH-type NN model introduced here was successful in the estimation of the residual turbidity with high accuracy in drinking water after water treatment process and the goodness of fit between the experimental and predicted result was calculated in statistical values (see Table 7).

The modeling results showed that turbidity, aluminum sulfate and poly electrolyte dosage and temperature, respectively, are more effective on turbidity removal in laboratory unit. Also in operation unit,secondary chlorination and aluminum sulfate dosage, suspended solids, pH, temperature are more effective on turbidity removal, respectively.

In addition, coagulants dosage and their effect on turbidity removal are optimized in optimum condition. Accordingly, the residual turbidity is minimized in moderate coagulants dosages. Also, in optimum conditions, the amount of aluminum sulfate injection is more effective than polyelectrolyte in turbidity removal.

Table 5
Polynomial equation of the GMDH-type NN model for prediction of residual turbidity in laboratory unit (jar tests)

First layer	Y_1	= 3.620088 – 0.213605*T + 0.01154937*Tu + 0.0062103*(T^2) + 0.0000027*(Tu^2) – 0.000935*(T*Tu)
	Y_2	= 4.493798 – 0.3020238*T – 0.036881*Al + 0.0073991*(T^2) + 0.0004491*(Al^2) + 0.0031474*(T*Al)
	Y_3	= 2.61378011 + 0.0054703*Tu – 0.13624851*Al + 0.000003145*(Tu^2) + 0.00612679*(Al^2) – 0.000336*(Al*Tu)
	Y_4	= 8.004829 – 0.44043292*T – 37.0172892*PE + 0.006584*(T^2) + 56.637658*(PE^2) + 1.42300963*(T*PE)
	Y_5	= –4.785646 – 0.50405*pH + 189.5744*PE + 0.1748844*(pH^2) + 15.029752*(PE^2) – 24.116636*(pH*PE)
	Y_6	= 3.6779063 + 0.042839*Al – 19.9460711*PE – 0.001806855*(Al^2) + 7.6689752*(PE^2) + 0.476306089*(Al*PE)
	Y_7	= 2.51981035 + 0.0037881*Tu – 4.72508*PE – 0.000004341*(Tu^2) – 1.5332369*(PE^2) + 0.00777722*(Tu*PE)
	Y_8	= 2.019251 + 0.0068211*Tu – 0.00023724 *EC – 0.00000426*(Tu^2) + 0.000000112*(EC^2) – 0.0000083637*(Tu*EC)
Second layer	Y_9	= 1.063341 – 5.336486*y1 + 5.283984*y2 + 1.01609457*(y1^2) – 1.11078037*(y2^2) + 0.342583*(y1*y2)
	Y_{10}	= –93.49988 + 22.585002*pH + 5.625058*y3 – 1.31078191*(pH^2) + 0.49575*(y3^2) – 0.902465*(pH*y3)
	Y_{11}	= 0.62369798 + 0.8022266 *y2 – 0.0012975*EC + 0.00323897*(y2^2) + 0.0000004563*(EC^2) + 0.00027109*(y2*EC)
	Y_{12}	= –0.0349126 + 2.2317146*y4 – 1.3384845*y3 – 0.04506056*(y4^2) + 0.653867791*(y3^2) – 0.555779798*(y3*y4)
	Y_{13}	= 5.0708868 + 9.7106101*y5 – 13.52146587*y6 – 4.3313956651*(y5^2) + 1.615808385*(y6^2) + 3.84743351*(y5*y6)
	Y_{14}	= 1.696355 – 2.9230916*y3 + 2.50754177*y7 + 0.309785*(y3^2) – 0.8520506*(y7^2) + 0.825611051*(y3*y7)
	Y_{15}	= –5.37725882 – 0.01131864*Tu + 6.839543*y7 – 0.000003815*(Tu^2) – 1.574250997*(y7^2) + 0.00582892*(Tu*y7)
	Y_{16}	= 2.1913037 + 2.722788*y8 – 3.4401048*y3 + 0.1891146921*(y8^2) + 1.46692032*(y3^2) – 1.350184*(y8*y3)
Third layer	Y_{17}	= –1.4650023 + 2.196097265*y9 – 0.038918551*y10 + 0.2582055319*(y9^2) + 0.7389476*(y10^2) – 1.21700714*(y9*y10)
	Y_{18}	= – 0.999077 + 2.9980897*y11 – 1.160116*y12 – 1.15129376*(y11^2) – 0.0338089*(y12^2) + 1.02054071*(y11*y12);
	Y_{19}	= –0.23340097 + 2.45215828*y13 – 1.39753497*y14 – 0.7611915*(y13^2) + 0.0079549*(y14^2) + 0.78764849*(y13*y14)
	Y_{20}	= –1.12690386 + 0.0711456*y15 + 1.6499725*y16 – 0.42627*(y15^2) – 0.63785994*(y16^2) + 0.986825673*(y15*y16)
Fourth layer	Y_{21}	= –0.0778141 – 3.4012776 *y17 + 4.501644*y18 – 0.681653866*(y17^2) – 2.511087878*(y18^2) + 3.1712389*(y17*y18)
	Y_{22}	= –1.357722164 + 0.991506595*y19 + 1.0883681*y20 – 1.26170562*(y19^2) – 1.140559583*(y20^2) + 2.213275*(y19*y20)
Output	R·Tu	= –0.119160395 – 1.24228089*y21 + 2.3285623*y22 – 0.41656787*(y21^2) – 1.613975659*(y22^2) + 2.0322823*(y21*y22)

Table 6
Polynomial equation of the GMDH-type NN model for prediction of residual turbidity in operation unit

First layer	Y_1	= 0.57728148 + 0.052173628*Cl2 + 0.000784288*SS – 0.024552294*(Cl2^2) – 1.65923E – 06*(SS^2) + 0.000266118*(Cl2*SS)
	Y_2	= 0.171610339 + 0.468035096*Cl2 + 0.321452557*pH – 0.048337996*(Cl2^2) – 0.034121745*(pH^2) – 0.036244902*(Cl2*pH);
	Y_3	= –1.207428774 + 0.22544072*Cl2 + 0.938100622*Cl1 + 0.005550412*(Cl2^2) – 0.11315651*(Cl1^2) – 0.061237191*(Cl1*Cl2)
	Y_4	= 0.732057828 + 0.266909459*Cl2 – 0.02916711*T – 0.021649471*(Cl2^2) + 0.000909189*(T^2) – 0.007175554*(Cl2*T)
	Y_5	= –0.654055371 + 0.825981243*Cl1 – 3.913441556*PE – 0.10252987*(Cl1^2) + 19.35076485*(PE^2) – 0.310892199*(Cl1*PE)
	Y_6	= –1.269608013 – 5.70468E – 05*SS + 0.0572104445*Cl1 – 1.57071E – 06*(SS^2) – 0.145482079*(Cl1^2) + 0.000303825*(SS*Cl1)
	Y_7	= –14.94409223 + 0.646317978*Al + 3.052746022*pH + 0.000598494*(Al^2) – 0.139568945*(pH^2) – 0.080446106*(Al*pH)
	Y_8	= 0.228714613 + 0.040379545*Al + 0.015592868*T – 0.000192097*(Al^2) + 0.000140755*(T^2) – 0.001699199*(Al*T)
	Y_9	= 26.46058051 – 6.602643392*pH + 0.215095107*T + 0.424991174*(pH^2) + 0.000854228*(T^2) – 0.030040297*(pH*T)
Second layer	Y_{10}	= 0.707711925 – 2.244524487*y1 + 0.290937995*y2 – 0.27361888*(y1^2) – 2.194302506*(y2^2) + 5.314076149*(y1*y2)
	Y_{11}	= 1.53239867 – 3.876186936 *y3 – 0.004379448*SS + 3.688030611*(y3^2) – 2.01045E – 06*(SS^2) + 0.008157184*(y3*SS)
	Y_{12}	= 2.38519139 – 2.969124853*y1 – 0.13401382*Al – 0.296811341*(y1^2) – 0.001293324*(Al^2) + 0.270685207*(Al*y1)
	Y_{13}	= 2.972891592 – 8.544725363*y3 – 0.543178645*y2 + 2.693565414*(y3^2) – 4.19009038*(y2^2) + 9.91946538*(y3*y2)
	Y_{14}	= 2.719627769 – 2.382555689*y4 – 4.880321266*y5 – 0.808105046*(y4^2) + 1.325785894*(y5^2) + 5.720735262*(y4*y5)
	Y_{15}	= 3.758860508 – 4.749918932*y6 – 5.664565103*y7 + 0.282998315*(y6^2) + 0.552816175*(y7^2) + 7.766311352*(y6*y7)
	Y_{16}	= 1.861032764 – 0.017941395*Al – 3.53943076*y8 – 0.002578567*(Al^2) + 1.293979697*(y8^2) + 0.14614261*(y8*Al)
Third layer	Y_{17}	= 0.632840132 + 1.223917454*y10 – 2.320890232*y11 – 2.834688668*(y10^2) + 0.130303694*(y11^2) + 4.421272258*(y10*y11)
	Y_{18}	= 4.495835921 – 5.629580045*y12 – 7.800549948*y13 – 1.815180569*(y12^2) – 0.137603098*(y13^2) + 13.47522797*(y13*y12)
	Y_{19}	= 1.206056727 – 3.110930644*y14 + 0.86812281* y15 + 1.403321304*(y14^2) – 0.512789227*(y15^2) + 1.230170777*(y15*y14)
	Y_{20}	= 1.17973265 – 0.397657654*y16 – 2.559417052*y9 + 0.070215245*(y16^2) + 1.436198074*(y9^2) + 1.759937537*(y16*y9)
Fourth layer	Y_{21}	= –0.85291 + 2.530925113 *y17 + 1.03526996*y18 + 1.5575071*(y17^2) + 3.52117667*(y18^2) – 7.008254091*(y17*y18)
	Y_{22}	= –1.111566157 – 0.608809507*y19 + 4.718297405*y20 – 0.187316977*(y19^2) – 4.45943*(y20^2) + 2.5257021*(y19*y20)
Output	R·Tu	= –0.22921 + 0.681074538*y21 + 0.8398371*y22 + 0.875192*(y21^2) + 0.778501*(y22^2) – 1.929735*(y21*y22)

Table 7
Model statistics and information for predicting treated water turbidity

Model performance	Laboratory unit (Jar test)			Operation unit		
	Training	Testing	Total	Training	Testing	Total
MSE	0.0398	0.0425	0.040516	0.01356	0.01376	0.0136
NRMSE	0.0705	0.2343	0.071126	0.097027	0.1955	0.0972
AADP (%)	8.0345	8.6874	8.4338	14.8475	12.9517	14.282
SI	0.0975	0.1086	0.1014	2.705E-08	3.141E-08	4.867E-08
BIAS	3.22E-13	–0.0544	–0.0163	–1.946E-13	–0.02857	–0.0085
R^2	0.99101	0.98749	0.9905	0.97175	0.9715	0.9714

Table 8
Optimum values of effective parameters on removal of turbidity

Unit	Inputs									Output
	PE [ppm]	Alum [ppm]	Tu [NTU]	pH [–]	T []	EC [µs/cm]	SS [mg/lit]	CL1 [ppm]	CL2 [ppm]	R·Tu [NTU]
Laboratory	0.13	13.83	66.93	8.19	24.42	261.23	–	–	–	0
Operation	0.12	13.97	–	7.6	16.76	–	91	5.57	0.84	0

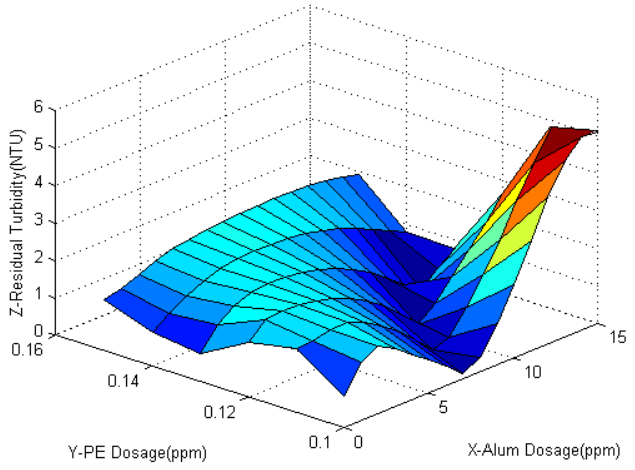

Fig. 7. Effect of aluminum sulfate and poly electrolyte dosage on residual turbidity in treated water in optimum condition of unit performance (jar tests).

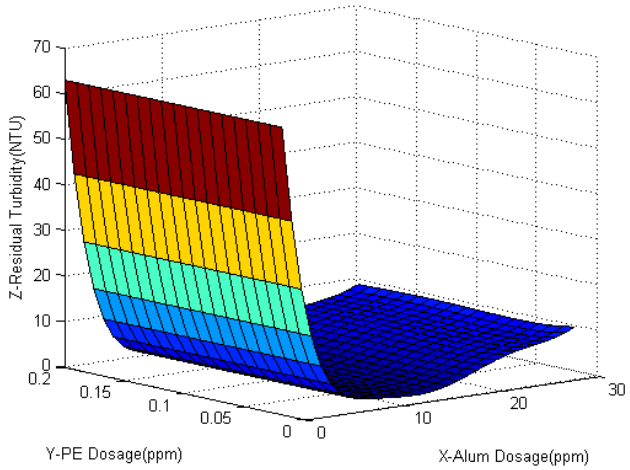

Fig. 8. Effect of aluminum sulfate and poly electrolyte dosage on residual turbidity in treated water in optimum condition of unit performance (operation unit).

The optimized model can be implemented online by integrating the existing control system available in Guilan drinking water treatment plant in Iran.

This model, however, is only based on the previous behavior of operators and jar-test results. Further work is needed to develop a model based on the dynamics of the system.

Acknowledgment

The authors of this paper would like to express their heartfelt appreciation of Guilan WTP, Iran, authorities for their valuable time and cooperation.

Symbols

T	—	Temperature [°C]
pH	—	Power of Hydrogen [-]
Tu	—	Turbidity [NTU]
SS	—	Suspended solids [mg/l]
EC	—	Electrical conductivity [µs/cm]
Cl1	—	Preliminary chlorination [ppm]
Cl2	—	Secondary chlorination [ppm]
Al , Alum	—	Aluminum sulfate [ppm]
PE, Poly	—	Poly electrolyte [ppm]
n	—	Number of variables
X_i	—	Inputs to model

a_i — Volterra series coefficients
Y_i — Output of model
$Y_{i,exp}$ — Experimental data
$Y_{i,model}$ — Model data
$Y_{exp,\ min}$ — Minimum of experimental data
$Y_{exp,\ max}$ — Maximum of experimental data
$\overline{Y}_{exp}$ — Average of experimental data
$\overline{Y}_{model}$ — Average of model data
N — Number of data samples

References

[1] P. Juntunen, M. Liukkonen, M. Pelo, M.J. Lehtola, Y. Hiltunen, Modelling of water quality: an application to a water treatment process, Appl. Comp. Intel. Soft Comp., 2012 (2012) 4.
[2] F. Edition, Guidelines for drinking-water quality, WHO Chron, 38 (2011) 104–108.
[3] R.D. Letterman, A.W.W. Association, Water Quality and Treatment, McGraw-Hill, 1999.
[4] M.L. Davis, Water and Wastewater Engineering, Design Principles and Practice, The Mc Graw-Hill Companies, Michigan State University,2010.
[5] F.-P.-T. C. o. D. Water, Turbidity in Drinking Water ed. Canada: Federal-Provincial-Territorial Committee 2012.
[6] G. Apostol, R. Kouachi, I. Constantinescu, Optimization of coagulation-flocculation process with aluminum sulfate based on response surface methodology, UPB Sci. Bull, Series B, 73 (2011) 77–84.
[7] L.S. Kang, J.L. Cleasby, Temperature effects on flocculation kinetics using Fe (III) coagulant, J. Environ. Eng., 121 (1995) 893.
[8] J.E. Van Benschoten, J.K. Edzwald, Chemical aspects of coagulation using aluminum salts—I. Hydrolytic reactions of alum and polyaluminum chloride, Water Res., 24 (1990) 1519–1526.
[9] J.E. Van Benschoten, J.K. Edzwald, Chemical aspects of coagulation using aluminum salts—II. Coagulation of fulvic acid using alum and polyaluminum chloride, Water Res., 24 (1990) 1527–1535.
[10] C. Huang, H. Shiu, Interactions between alum and organics in coagulation, Colloids Surf. A Physicochem. Eng. Asp., 113 (1996) 155–163.
[11] J. Xie, D. Wang, J. van Leeuwen, Y. Zhao, L. Xing, C.W. Chow, pH modeling for maximum dissolved organic matter removal by enhanced coagulation, J. Environ. Sci., 24 (2012) 276–283.
[12] S. Heddam, A. Bermad, N. Dechemi, ANFIS-based modelling for coagulant dosage in drinking water treatment plant: a case study, Environ. Monit. Assess., 184 (2012) 1953–1971.
[13] J. Bratby, Coagulation and Flocculation in Water and Wastewater Treatment, IWA Publishing, 2016.
[14] H.R. Maier, N. Morgan, C.W. Chow, Use of artificial neural networks for predicting optimal alum doses and treated water quality parameters, Environ. Model Softw., 19 (2004) 485–494.
[15] Y. Zhao, Y. Wang, B. Gao, H. Shon, J.-H. Kim, Q. Yue, Coagulation performance evaluation of sodium alginate used as coagulant aid with aluminum sulfate, iron chloride and titanium tetrachloride, Desalination, 299 (2012) 79–88.
[16] S. Xia, X. Li, Q. Zhang, B. Xu, G. Li, Ultrafiltration of surface water with coagulation pretreatment by streaming current control, Desalination, 204 (2007) 351–358.
[17] J.C. Vickers, M.A. Thompson, U.G. Kelkar, The use of membrane filtration in conjunction with coagulation processes for improved NOM removal, Desalination, 102 (1995) 57–61.
[18] R. Bryant, Optimizing coagulation with the Streaming Current Monitor, J. New England Water Works Assoc., 110 (1996) 268–271.
[19] C. Baxter, S. Stanley, Q. Zhang, Development of a full-scale artificial neural network model for the removal of natural organic matter by enhanced coagulation, J. Water SRT., 48 (1999) 129–136.
[20] R.-F. Yu, S.-F. Kang, S.-L. Liaw, M.-C. Chen, Application of artificial neural network to control the coagulant dosing in water treatment plant, Water Sci. Technol., 42 (2000) 403–408.
[21] J.M. Montgomery, Water Treatment: Principles and Design, Published by John Wiley & Sons Ltd, New York, USA, 1985.
[22] D.-S. Joo, D.-J. Choi, H. Park, The effects of data preprocessing in the determination of coagulant dosing rate, Water Res., 34 (2000) 3295–3302.
[23] J.-L. Lin, C. Huang, J.R. Pan, D. Wang, Effect of Al (III) speciation on coagulation of highly turbid water, Chemosphere, 72 (2008) 189–196.
[24] J.H. Kweon, H.-W. Hur, G.-T. Seo, T.-R. Jang, J.-H. Park, K.Y. Choi, *et al.*, Evaluation of coagulation and PAC adsorption pretreatments on membrane filtration for a surface water in Korea: A pilot study, Desalination, 249 (2009) 212–216.
[25] C. Gagnon, B. Grandjean, J. Thibault, Modelling of coagulant dosage in a water treatment plant, Artif. Intellig. Eng., 11 (1997) 401–404.
[26] G. Carrera, J. Aires-de-Sousa, Estimation of melting points of pyridinium bromide ionic liquids with decision trees and neural networks, Green Chem., 7 (2005) 20–27.
[27] G.-D. Wu, S.-L. Lo, Predicting real-time coagulant dosage in water treatment by artificial neural networks and adaptive network-based fuzzy inference system, Eng. Appl. Artif. Intell., 21 (2008) 1189–1195.
[28] A. Robenson, S. Shukor, N. Aziz, Development of process inverse neural network model to determine the required alum dosage at Segama Water Treatment Plant Sabah, Malaysia, Comp. Aided Chem. Eng., 27 (2009) 525–530.
[29] K.H. Reckhow, Water quality prediction and probability network models, Can. J. Fish Aquat. Sci., 56 (1999) 1150–1158.
[30] C. Baxter, Q. Zhang, S. Stanley, R. Shariff, R.-R. Tupas, H. Stark, Drinking water quality and treatment: the use of artificial neural networks, Can. J. Civ. Eng., 28 (2001) 26–35.
[31] W.A. Pike, Modeling drinking water quality violations with Bayesian networks, J. Am. Water Resour. Assoc., 40 (2004) 1563–1578.
[32] M. Najafzadeh, Neurofuzzy-based GMDH-PSO to predict maximum scour depth at equilibrium at culvert outlets, J. Pipeline Syst. Eng. Pract., 7 (2015) 06015001.
[33] M. Najafzadeh, Neuro-fuzzy GMDH systems based evolutionary algorithms to predict scour pile groups in clear water conditions, Ocean Eng., 99 (2015) 85–94.
[34] M. Najafzadeh, H. Bonakdari, Application of a neuro-fuzzy GMDH model for predicting the velocity at limit of deposition in storm sewers, J. Pipeline Syst. Eng. Pract., 8 (2016) 06016003.
[35] M. Najafzadeh, F. Saberi-Movahed, S. Sarkamaryan, NF-GMDH-Based self-organized systems to predict bridge pier scour depth under debris flow effects, Marine Georesour. Geotechnol., (2017) 1–14.
[36] M. Najafzadeh, A. Tafarojnoruz, Evaluation of neuro-fuzzy GMDH-based particle swarm optimization to predict longitudinal dispersion coefficient in rivers, Environ. Earth Sci., 75 (2016) 157.
[37] M. Najafzadeh, G.-A. Barani, M.R.H. Kermani, Abutment scour in clear-water and live-bed conditions by GMDH network, Water Sci. Technol., 67 (2013) 1121–1128.
[38] M. Najafzadeh, G.-A. Barani, Comparison of group method of data handling based genetic programming and back propagation systems to predict scour depth around bridge piers, Scientia Iranica, 18 (2011) 1207–1213.
[39] M. Najafzadeh, H.M. Azamathulla, Group method of data handling to predict scour depth around bridge piers, Neural Comput. Applic., 23 (2013) 2107–2112.
[40] M. Najafzadeh, G.-A. Barani, M.-R. Hessami-Kermani, Group method of data handling to predict scour at downstream of a ski-jump bucket spillway, Earth Sci. Inform., 7 (2014) 231–248.
[41] A. Daghbandan, M. Akbarizadeh, M. Yaghoobi, Modeling and optimization of poly electrolyte dosage in water treatment process by GMDH type-NN and MOGA, Int. J. Chemoinform. Chem. Eng. (IJCCE), 3 (2013) 94–106.
[42] A.G. Ivakhnenko, Polynomial theory of complex systems, IEEE Trans. Syst. Man. Cybern., 1 (1971) 364–378.

[43] S. Farlow, Self-organizing method in modeling: GMDH type algorithm, ed: Marcel Dekker Inc., New York, 1984.
[44] A.G. Ivakhnenko, Polynomial theory of complex systems, Trans. Syst. Man. Cybern., 1 (1971) 364–378.
[45] N. Nariman-Zadeh, A. Darvizeh, M. Felezi, H. Gharababaei, Polynomial modelling of explosive compaction process of metallic powders using GMDH-type neural networks and singular value decomposition, Model Simul. Mat. Sci. Eng., 10 (2002) 727.
[46] A. Jamali, A. Hajiloo, N. Nariman-Zadeh, Reliability-based robust Pareto design of linear state feedback controllers using a multi-objective uniform-diversity genetic algorithm (MUGA), Expert Syst. Applic., 37 (2010) 401–413.
[47] A. Jamali, N. Nariman-zadeh, H. Ashraf, Z. Jamali, Robust Pareto Design of ANFIS Networks for Nonlinear Systems with Probabilistic Uncertainties, 2011, pp. 300–304.
[48] A. Jamali, N. Nariman-zadeh, K. Atashkari, Multi-objective uniform-diversity genetic algorithm (MUGA), Adv. Evolution. Algorithms, (2008) 978–983.
[49] N. Nariman-Zadeh, A. Darvizeh, M. Dadfarmai, Design of ANFIS networks using hybrid genetic and SVD methods for the modelling of explosive cutting process, J. Mater. Process. Technol., 155 (2004) 1415–1421.
[50] M. Najafzadeh, F. Saberi-Movahed, GMDH-GEP to predict free span expansion rates below pipelines under waves, Marine Georesour. Geotechnol., (2018) 1–18.